

15.1;05.5;11.4

Superconducting noise-source for ultra-low temperatures

© T.M. Kim¹, S.V. Shitov^{1,2}

¹ National University of Science and Technology „MISIS“, Moscow, Russia

² Kotelnikov Institute of Radio Engineering and Electronics, Russian Academy of Sciences, Moscow, Russia

E-mail: kim.tatyana.mail@gmail.com

E-mail: sergey3e@gmail.com

Received June 1, 2021

Revised July 21, 2021

Accepted September 12, 2021

The device operates at temperatures < 300 mK and comprises a hafnium microbridge and a superconducting aluminum tunnel junction both integrated into a common coplanar waveguide. The microbridge matches with a planar antenna and operates as an optical blackbody at frequencies 600–700 GHz. The coplanar terminal is the blackbody output in the 1–2 GHz frequency range. The microbridge temperature can be set in the range of 0.4–9 K and calibrated using the shot noise of the tunnel junction. Temperature modulation of each of the sources can be performed independently using a direct current which transit them from the superconducting to the normal state with characteristic times < 0.1 ms and heating power $\sim 1 \mu\text{W}$.

Keywords: Superconducting microbridge, superconducting tunnel junction, thermodynamic noise, shot noise, noise thermometry.

DOI: 10.21883/TPL.2022.15.55282.18897

Noise measurements at ultra-low temperatures (30–300 mK) are necessary for calibration of ultra-sensitive thermal detectors for space exploration in the terahertz (THz) range [1] and for amplifiers of quantum information processing circuits in the gigahertz (GHz) range [2]. The existing blackbody emitter (BBE) methods use constant [3] or pulsed [4] heating of BBE with a power of ~ 1 mW, which may be critical for a dilution refrigerator with a cooling capacity of $\sim 100 \mu\text{W}$. In the study [5] BBE [4] is characterized as a structural analogue of a composite bolometer with a size of $\sim 10 \times 10$ mm and mass of ~ 0.1 g, heated with the voltage pulses ~ 10 V that cause heating of the film absorber with the front rise ~ 1 ms. This allows to calibrate the sensitivity and reaction rate of the image matrices [5]. However, the effective cycle time of heating–cooling of such a source is $\tau \sim 2$ s, which makes it difficult to implement a radiometer with modulation frequencies $f_m > 1$ Hz: at $f_m \sim 10$ Hz, the temperature amplitude of BBE decreases $\sim (\tau f_m)^{-1}$. In this paper, the electrophysical model and the design of the integrated circuit of a noise calibrator are analyzed, the advantages of which are low thermal power ($\sim 1 \mu\text{W}$) and short thermal relaxation time ($\tau < 0.1$ ms). The proposed BBE also resembles a bolometer, but it is based on a resistive microbridge and a planar THz-antenna. The range of noise temperatures of the calibrator 0.4–9 K is optimal for the study of THz-detectors exposed to a cosmic microwave background with a temperature of $T_{bg} \approx 2.7$ K. The physical temperature T of the film resistor can be set either by heating the substrate or by a current heating the film relative to the substrate. The first method is implemented in BBE [4], the second requires the data for the local temperature of the film, which is impossible neither with

the use of standard cryogenic thermometers [6], nor with the use of integral structures of the type [4]. It is proposed to measure the temperature of a microresistor by comparing its noise at GHz-frequencies with the shot noise of a SIS (superconductor–insulator–superconductor) tunnel junction [7,8], and use this temperature to calculate thermodynamic noise at THz frequencies, which is the advancement in methods of noise thermometry [9]. The schematic diagram of the device is shown in Fig. 1. Two noise sources are connected in series to a common electrical circuit on one chip. A reference power meter is connected to the output of the chip — a cooled detector or a low-noise cooled amplifier in radiometric mode with an instantaneous band of 1 GHz and a noise temperature of ~ 10 K. The superconducting and resistive states of the microbridge and the SIS junction allow the following: 1) turn off any source via switching it to a superconducting state; 2) transmit a lossless signal from the selected source; 3) independently control the noise level using bias current in a wide frequency range (up to ~ 100 kHz); 4) use critical temperatures of materials as reference parameters.

The noise power P_n of an ideal resistor can be described by Planck’s formula in an unlimited frequency range Δf . In the limit of low frequencies or high temperatures ($hf \ll k_B T$, where h — Planck constant, f — frequency, k_B — Boltzmann constant) the noise power transmitted to the load, $P_n = k_B T \Delta f$. Under the condition $eV \gg k_B T \gg hf$ (where e — electron charge, V — voltage), shot noise dominates in the SIS-junction, which depends on the current I . The square of the shot noise voltage $\langle V_{shot}^2 \rangle = 2eIR_n^2 \Delta f$, where R_n — normal resistance, whence the matched power $P_{shot} = eIR_n \Delta f / 2$. The equivalent temperature of shot noise $T_{shot} = P_{shot} / 2k_B \Delta f$

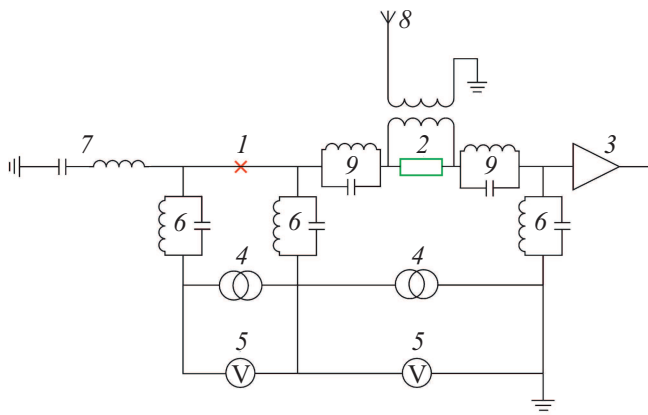


Figure 1. Schematic diagram of the device. 1 — SIS junction, 2 — superconducting microbridge, 3 — reference power meter, 4 — current sources, 5 — voltmeters, 6 — band-stop filters in the range 1–2 GHz, 7 — band-pass filter 1–2 GHz, 8 — double-slot THz antenna, 9 — band-stop antenna filters 600–700 GHz.

is proportional to I on the linear branch of the current-voltage characteristic (IV-curve) (Fig. 2, *a*), the minimum value of $T_{shot\ min} = eV_g/2k_B$. For a SIS junction made of aluminum $V_g = 340\text{--}360\ \mu\text{V}$, heat dissipation $\sim 2\ \text{nW}$ and $T_{shot\ min} \approx 2\ \text{K}$. The shot noise frequency range Δf_{SIS} of the SIS junction with an area of $10\ \mu\text{m}^2$ does not exceed 50 GHz according to the condition $2\pi\Delta f_{SIS}R_nC_{SIS} < 1$, where C_{SIS} — the capacity of the SIS junction. In addition to direct noise comparison, the thermal hysteresis method of the VAC microbridge IV-curve [10] can be used (fig. 2, *b*). The current rise above the critical current I_c leads to a voltage jump, and the microbridge becomes a resistor R_n , heated to a temperature T , which must exceed the temperature of the substrate T_0 . The switch back to the superconducting state is realized at the return current $I_r < I_c$, while T decreases to the critical value T_c , and the

heating — to $P_r = I_r^2 R_n$. At $T < 1\ \text{K}$, it is necessary to take into account the effect of the electron gas [11] and use the electron temperature T_e as the fluctuation temperature, which can be found by solving the equation of constant heat flow through the electron-phonon and phonon-phonon interfaces

$$P_{e-ph}(T) = \Sigma v (T_e^n - T_k^n) = \frac{S}{A} (T_k^4 - T_0^4), \quad (1)$$

where T_k — lattice temperature, Σ — electron-phonon interaction constant of the material, v — bridge volume, $n = 5\text{--}6$, A — Kapitsa constant [12], S — the area of thermal contact of the film with the substrate. The right side of the equation (1) reflects the heating of the phonon system of the film relative to the phonon system of the substrate; at temperatures above 1 K $T_k - T_0 \gg T_e - T_k$. The power coefficient n can be verified by measuring the thermal power at the lowest point of the resistive branch of the IV-curve, where $P_{e-ph}(T) = I_r(T_0)^2 R_n$. At this point, the calculated noise of the microbridge should correspond to the shot noise: $T_e \approx T_{shot}$. The noise spectrum of a bridge with an electron gas can be considered as thermodynamical up to frequencies limited by the efficiency of Andreev mirrors [13] at the interface between bridge and superconducting niobium electrodes, i.e. up to $\sim 750\ \text{GHz}$. BBE is designed for use in two frequency bands (1–2 and 600–700 GHz) to continue the projects [1,15]. The temperature range of the microbridge is limited by the critical temperatures of hafnium and niobium: $T_{cHf} \approx 0.4\ \text{K}$ and $T_{cNb} \approx 9\ \text{K}$. The simplified layout of the chip is shown in Fig. 3, *a*: the SIS junction and the microbridge are integrated into a common coplanar line made of niobium on a sapphire substrate. The microbridge is matched simultaneously with a double-slot THz antenna [1,15,16] and a reference amplifier connected with a coplanar waveguide in the range of 1–2 GHz. Band-stop filters of antenna prevent signal leak in the range of 600–700 GHz and are transparent in

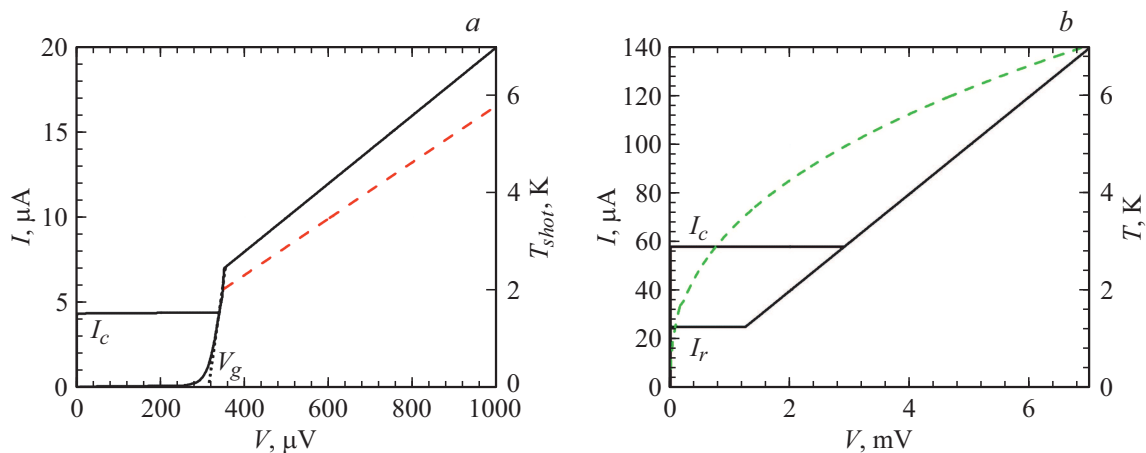


Figure 2. Characteristics of noise sources. *a* — The IV-curve of a SIS tunnel junction (solid line) and the noise temperature T_{shot} calculated above the gap voltage V_g (dashed line); *b* — hysteresis IV-curve of a superconducting microbridge (solid line) and the physical temperature T , calculated taking into account the strong temperature dependence of the heat sink (dashed line).

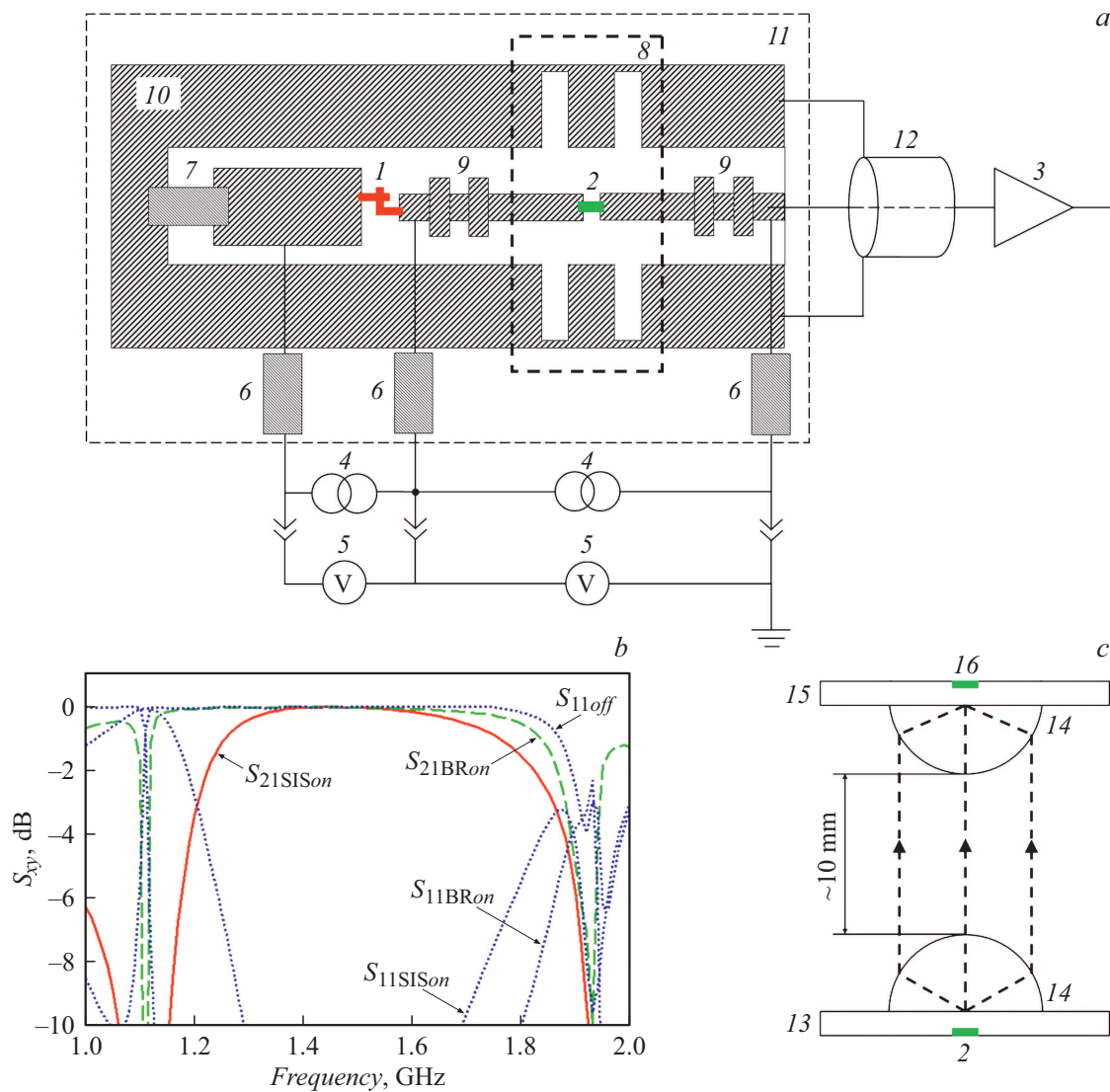


Figure 3. Device design. *a* — simplified chip topology and external circuits; chip metallization is shaded. 1–9 — same as in Fig. 1, 10 — coplanar waveguide, 11 — dielectric substrate, 12 — coaxial cable. *b* — calculated [14] parameters of the experimental chip: the signal transmission coefficient from the SIS junction ($S_{21SISon}$), the transmission coefficient from the microbridge (S_{21BRon}), the reflection coefficient when the corresponding source is „off“ (S_{11off}) and „on“ ($S_{11SISon}$, S_{11BRon}). *c* — signal transmission scheme of BBE using collimating immersion optics for the project [1]: the reference amplifier 3 is connected to the chip 13 on which the emitter 2 is located; lens 14 forms a collimated beam, which enters through a similar lens to the chip 15, where the detector under test 16 is located.

the range of 1–2 GHz. Current sources and voltmeters are connected via band-stop filters 1–2 GHz. Electrodynamics modeling of the chip in the Cadence AWR [14] confirmed the feasibility of the proposed device in the range of 1–2 GHz (Fig. 3, *b*). The chip is placed on a flat surface of an elliptical immersion lens (Fig. 3, *c*) so that the antenna is in its focus, and the tested detector [15], equipped with a similar lens antenna (LA), is located at a distance of ~ 10 mm in the near field zone, where the radiation front is flat. Such an LA system with a typical directivity coefficient of > 20 dB does not require intermediate optics and provides high EMI immunity: the attenuation of off-axis beams will be > 16 dB. Signal losses are determined by diffraction scattering at the LA aperture and do not

exceed 1 dB ($\sim 20\%$). The thermodynamic background of the cryostat at 0.3 K is characterized by a Planck spectrum boundary at about 10 GHz that allows to neglect the photon load of the THz detector. Microresistor 50Ω size $2 \times 2 \times 0.05 \mu\text{m}$ with thermal conductivity $G = 10^{-9}$ W/K heats up to $T = 9$ K by a power of $3 \mu\text{W}$ at a bias of 13 mV; for a calibration temperature of 2 K, the power drops down to 2 nW at a voltage of 0.3 mV. To estimate the parasitic heating ΔT of a sapphire substrate with a specific thermal conductivity $G_s = 10^{-2}$ W/(K · m) at $T_0 = 100$ mK [17], it is possible to use a simplified model of heat flow in the form of an isothermal hemisphere diameter of D . The ratio $\Delta T(D) = P/G_s \pi D$ is the result of integration of the temperature gradient between a power source P diameter

D towards an infinitely distant isothermal hemisphere T_0 . If the SIS junction is placed at 2 mm from the bridge, then $\Delta T < 10$ mK can be calculated at this point, and such heating of the SIS junction can be neglected. The above estimates demonstrate that the proposed noise source might not overload the dilution cryostat and, in principle, can be integrated as part of a microcircuit with a practical bolometer and/or amplifier. The modulation experiment in the project [15] allowed to estimate the temperature relaxation time of a hafnium microbridge $< 10 \mu\text{s}$ that is determined by the electron-phonon relaxation time.

The use of an electron gas as a thermodynamic environment [18] opens new possibilities in precision measurements of ultra-low-noise devices.

Funding

The work was carried out with the financial support of the Russian Foundation for Basic Research within the framework of the scientific project № 20-37-90094, as well as the Ministry of Education and Science of the Russian Federation within the framework of the NUST MISIS Competitiveness Improvement Program in Materials science — NUST MISIS grant № K2-2020-016.

Conflict of interest

The authors declare that they have no conflict of interest.

References

- [1] A.V. Merenkov, V.I. Chichkov, A.B. Ermakov, A.V. Ustinov, S.V. Shitov, *IEEE Trans. Appl. Supercond.*, **28** (7), 1 (2018). DOI: 10.1109/TASC.2018.2827981
- [2] B.H. Eom, P.K. Day, H.G. LeDuc, J. Zmuidzinas, *Nature Phys.*, **8**, 623 (2012). DOI: 10.1038/nphys2356
- [3] A.V. Uvarov, S.V. Shitov, A.N. Vystavkin, *Meas. Techn.*, **53** (9), 1047 (2010). DOI: 10.1007/s11018-010-9617-4
- [4] Ph. Abbon, A. Delbart, M. Fesquet, C. Magneville, B. Mazeau, J.-P. Pansart, D. Yvon, L. Dumoulin, S. Marnieros, Ph. Camus, T. Durand, Ch. Hoffmann, *Nucl. Instrum. Meth. Phys. Res. A*, **575** (3), 412 (2007). DOI: 10.1016/j.nima.2007.02.094
- [5] S. Masi, P. de Bernardis, A. Paiella, F. Piacentini, L. Lamagna, A. Coppolecchia, P.A.R. Ade, E.S. Battistelli, M.G. Castellano, I. Colantoni, F. Columbro, G. D'Alessandro, M. De Petris, S. Gordon, C. Magneville, P. Mauskopf, G. Pettinari, G. Pisano, G. Polenta, G. Presta, E. Tommasi, C. Tucker, V. Vdovin, A. Volpe, D. Yvon, *J. Cosmol. Astropart. Phys.*, **2019** (7), 003 (2019). DOI: 10.1088/1475-7516/2019/07/003
- [6] <https://www.lakeshore.com/products/categories/temperature-products/cryogenic-temperature-sensors>
- [7] V.Yu. Belitsky, V.P. Koshelets, I.L. Serpuchenko, M.A. Tarasov, L.V. Filippenko, S.V. Shitov, in *Proc. of the 20th Eur. Microwave Conf.* (IEEE, 1990), vol. 1, p. 816. DOI: 10.1109/EUMA.1990.336144
- [8] H. Inoue, T. Noguchi, K. Kohno, *J. Phys.: Conf. Ser.*, **234**, 042014 (2010). DOI: 10.1088/1742-6596/234/4/042014
- [9] L. Spietz, R.J. Schoelkopf, P. Pari, *Appl. Phys. Lett.*, **89** (18), 183123 (2006). DOI: 10.1063/1.2382736
- [10] B.S. Karasik, S.V. Pereverzev, D. Olaya, J. Wei, M.E. Gershenson, A.V. Sergeev, *IEEE Trans. Appl. Supercond.*, **19** (3), 532 (2009). DOI: 10.1109/TASC.2009.2019426
- [11] F.C. Wellstood, C. Urbina, J. Clarke, *Phys. Rev. B*, **49** (9), 5942 (1994). DOI: 10.1103/PhysRevB.49.5942
- [12] G.L. Pollack, *Rev. Mod. Phys.*, **41** (1), 48 (1969). DOI: 10.1103/RevModPhys.41.48
- [13] D. Chouvaev, L. Kuzmin, M. Tarasov, *Supercond. Sci. Technol.*, **12** (11), 985 (1999). DOI: 10.1088/0953-2048/12/11/386
- [14] Cadence AWR [Electronic resource]. URL: <https://www.awr.com/awr-software/products/awr-design-environment>
- [15] A.V. Merenkov, S.V. Shitov, V.I. Chichkov, A.B. Ermakov, T.M. Kim, A.V. Ustinov, *Tech. Phys. Lett.*, **44** (7), 581 (2018). DOI: 10.1134/S106378501807012X
- [16] S.V. Shitov, *Tech. Phys. Lett.*, **37** (10), 932 (2011). DOI: 10.1134/S1063785011100117
- [17] A.L. Woodcraft, M. Barucci, P.R. Hastings, L. Lolli, V. Martelli, L. Risegari, G. Ventura, *Criogenics*, **49** (5), 159 (2009). DOI: 10.1016/j.cryogenics.2008.10.024
- [18] B.S. Karasik, C.B. McKitterick, T.J. Reck, D.E. Prober, *IEEE Trans. Terahertz Sci. Technol.*, **5** (1), 16 (2015). DOI: 10.1109/TTHZ.2014.2370755